

## Crystalline fragments in glasses

Giomal A. Antonio

*Departamento de Física, Universidade Estadual Paulista–Bauru, Caixa Postal 473, 17033 Bauru, São Paulo, Brazil*

Rajiv K. Kalia, Aiichiro Nakano, and Priya Vashishta

*Concurrent Computing Laboratory for Materials Simulations and Department of Physics and Astronomy,  
Louisiana State University, Baton Rouge, Louisiana 70803-4001*

(Received 22 July 1991)

The nature of tetrahedral molecular fragments is investigated in  $\text{SiSe}_2$  glasses using the molecular-dynamics method. The glass consists of both edge-sharing (ES) and corner-sharing tetrahedra. The ES tetrahedra are the building blocks of chain-like-molecular fragments. The two-edge-sharing tetrahedra are the nucleus, and corner-sharing configurations provide connecting hinges between fragments. Statistics of rings and fragments reveals that threefold and eightfold rings are most abundant, chainlike fragments that are typically 10–15 Å long occur mostly in eightfold rings, and the longest fragments occur in elevenfold rings.

Silicon diselenide has an unusual crystal structure. The local structural units are  $\text{Si}(\text{Se}_{1/2})_4$  tetrahedra, each of which is bonded at two edges.<sup>1</sup> Such configurations form molecular entities that are non-intersecting infinite chains of edge-sharing (ES) tetrahedra. In contrast, crystalline  $\text{GeSe}_2$  consists of two-dimensional planes that are made of both corner-sharing (CS) and edge-sharing tetrahedra,<sup>2</sup> and crystalline forms of  $\text{SiO}_2$  and  $\text{GeO}_2$  are three-dimensional networks of only corner-sharing tetrahedra.<sup>3</sup> In the amorphous state, the structures of  $a$ - $\text{SiSe}_2$ , (Ref. 4)  $a$ - $\text{GeSe}_2$  (Ref. 5),  $a$ - $\text{SiO}_2$  (Ref. 6), and  $a$ - $\text{GeO}_2$  (Ref. 7) have been determined by neutron and x-ray diffraction experiments, and the presence of a tetrahedral unit has been established in all these systems. The determination of the nature of larger molecular entities, e.g., tetrahedral molecular fragments or crystalline fragments, requires the knowledge of angular correlations. These correlations cannot be determined from diffraction data on glasses, since only the spherically averaged static structure factor,  $S(|q|)$ , is measured in these experiments. Furthermore, when the structure factor in the amorphous states of these systems is plotted in reduced units,  $S(Q)$  versus  $Q = |q|d_s$  [ $d_s = (6/\pi\rho)^{1/3}$ ;  $\rho$  is the number density], the data for all the four systems show the first sharp diffraction peak at  $Q \approx 4.5$ .<sup>8</sup> Therefore, the nature of microscopic order in the amorphous state, which is clearly different in these systems due to different interatomic interactions manifested in their qualitatively different crystal structures, cannot be inferred from  $S(Q)$  alone. Infrared,<sup>9</sup> Raman,<sup>10–12</sup> and NMR measurements<sup>13,14</sup> can be used to study local environments of atoms and elementary structural units. When combined with diffraction data, these experimental probes can provide structural information about larger molecular entities and crystalline fragments in glasses.

In this paper, we investigate the nature of tetrahedral molecular fragments in  $a$ - $\text{SiSe}_2$  using the molecular dynamics (MD) method. Molecular dynamics simulations reveal that unlike the crystalline phase, where every tetrahedron shares two edges,  $a$ - $\text{SiSe}_2$  consists of half the

tetrahedra in CS configurations and the remaining tetrahedra share edges. Among the ES tetrahedra, 89% share one edge and the remaining 11% share two edges. ES tetrahedra are the building blocks of tetrahedral-molecular fragments, where two-edge-sharing tetrahedra are the nucleus and CS configurations provide the connecting hinges between the molecular fragments. Analysis of rings and fragments in  $a$ - $\text{SiSe}_2$  reveals that (1) threefold and eightfold rings are most abundant, (2) chainlike fragments occur predominantly in eightfold rings, and (3) the longest fragments occur in elevenfold rings. These chainlike fragments are typically 10–15 Å long.

Molecular dynamics simulations were performed on 648- and 5184-particle systems with periodic boundary conditions. For the 648-particle system, the simulations were performed in a cubic box of 27.380 Å (28.102 Å) at the experimental density of 3.25 g/cm<sup>3</sup> (3.01 g/cm<sup>3</sup>) for the glass (liquid).<sup>4</sup> The larger system was simulated to estimate the finite-size effects. The effective potential in these calculations is a sum of two-body,  $V_2(|\mathbf{r}_i - \mathbf{r}_j|)$ , and three-body,  $V_3(\mathbf{r}_i, \mathbf{r}_j, \mathbf{r}_k)$ , interactions.<sup>15</sup> The two-body interaction includes steric repulsions, Coulomb potential due to charge transfer from Si to Se, and a charge-dipole term to take into account the large electronic polarizability of  $\text{Se}^{2-}$ . The three-body potentials for Se-Si-Se and Si-Se-Si interactions include bond stretching and bond bending terms.

Starting from a well thermalized molten state at 2000 K, the system was cooled to another molten state of 1293 K and thermalized for 30 000 time steps. At 1293 K, the constants of self-diffusion of Si and Se were  $0.95 \times 10^{-5}$  and  $0.96 \times 10^{-5}$  cm<sup>2</sup>/s, respectively. This system was quenched to 600 K, where it underwent thermal arrest. This amorphous state was thermalized for 60 000 time steps. Using this quenching-thermalization schedule, two other samples of computer glass were obtained at  $T = 293$  and 0 K.

A snapshot of a 9-Å-thick slice of a computer glass at  $T = 293$  K is shown in Fig. 1. The figure shows that in

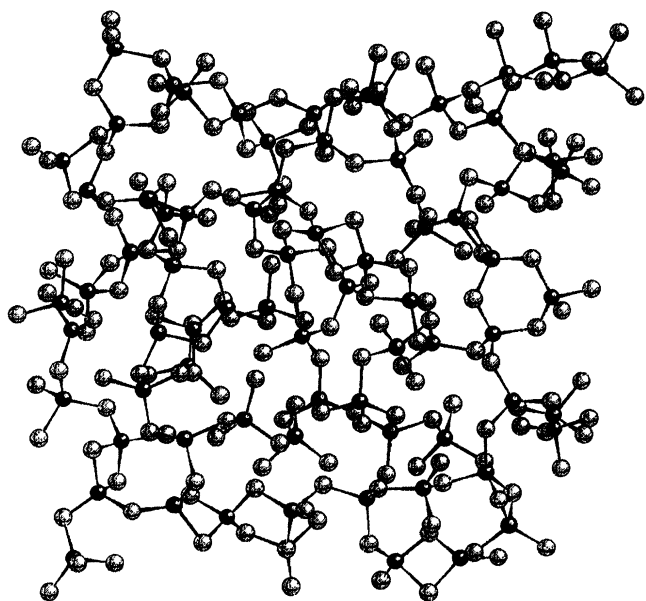


FIG. 1. Snapshot of a 9-Å-thick slice of a MD glass. Si atoms are indicated in blue and Se atoms in yellow.

the glass each Si has four nearest-neighbor Se atoms, so the local structural unit is a  $\text{Si}(\text{Se}_{1/2})_4$  tetrahedron. These local structural units are connected to one another to form rings of various sizes.

A neutron static structure factor,  $S_n(q)$ , calculated from MD trajectories is shown along with the experimental results<sup>4</sup> in Fig. 2. It is clear that the results of the simulation are in good agreement with the diffraction data. From the radial distribution functions, we determine that the Si-Se and Se-Se bond lengths are 2.28 Å and 3.73 Å, respectively, which are in good agreement with the corresponding experimental values of 2.30 Å and 3.80 Å.<sup>4</sup> This establishes that our simulation of  $\alpha$ - $\text{SiSe}_2$  is a satisfactory representation of the experimental system.

To examine distortions of tetrahedra and their connectivity, we have calculated Se-Si-Se and Si-Se-Si bond-angle distributions in the glass. For an ideal tetrahedron the Se-Si-Se angle is 109°. In crystalline  $\text{SiSe}_2$ ,  $c$ - $\text{SiSe}_2$ , the Se-Si-Se angle has three values, 100.0°, 112.2°, and 116.7°, indicating distortions of tetrahedra, each of which shares two edges. Nearest-neighbor connectivity of tetrahedra is described by the Si-Se-Si bond-angle distribution. This

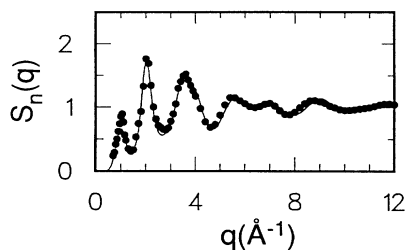


FIG. 2. Neutron static structure factor,  $S_n(q)$ , for  $\text{SiSe}_2$  glass at 293 K. The continuous line denotes the MD result, and solid circles are from the neutron diffraction measurements (Ref. 4).

angle has a value of 80° in  $c$ - $\text{SiSe}_2$ , indicating large distortions the tetrahedra have to undergo, while sharing two edges.<sup>1</sup> In  $c$ - $\text{GeSe}_2$ , which has edge- and corner-sharing tetrahedra, Ge-Se-Ge angle distribution has a peak at 94°, and individual tetrahedra have smaller distortions compared to those in  $c$ - $\text{SiSe}_2$ .<sup>2</sup> Figure 3 shows Se-Si-Se and Si-Se-Si distributions in  $\alpha$ - $\text{SiSe}_2$ . The two-peak structure of Se-Si-Se at 93° and 108° is a reflection of crystalline angles.<sup>1</sup> The Si-Se-Si distribution in  $\alpha$ - $\text{SiSe}_2$  also shows two peaks. The first at 86° has an analog in  $c$ - $\text{SiSe}_2$  and indicates ES tetrahedra, whereas the second peak at 111° is indicative of CS configurations in the glass. The ES configurations are also manifested in an interesting way in the Si-Si pair-distribution function,  $g_{\text{Si-Si}}(r)$ , in Fig. 4(a). There are two distinct peaks at 3.13 and 3.80 Å in  $g_{\text{Si-Si}}(r)$ . The first peak is entirely due to correlations arising from ES tetrahedra. Taking the Si-Si cutoff to be the distance at the minimum after the first peak (3.4 Å) of  $g_{\text{Si-Si}}(r)$ , we determine the bond-angle distributions Si-Si-Se shown in Fig. 4(b). Figure 4(c) is the same distribution with the Si-Si cutoff at 4.6 Å, which includes both peaks in Fig. 4(a). In Figs. 4(b) and 4(c) the red peaks at 47° arise from ES tetrahedra, i.e., two twofold rings. In Fig. 4(c) the blue peak at 35° is due to threefold rings.

The topology of covalent glasses is commonly discussed in terms of rings. We have calculated the distribution of twofold to twelfold rings from MD configurations. The distributions of rings for the crystal and glass are given in Table I. An  $n$ -fold ring is determined as follows: Each Si has four Se nearest neighbors and there are six Se-Si-Se paths. For each of these paths we determine the shortest closed ring. Therefore, an  $n$ -fold ring consists of  $2n$  alternating Si-Se bonds and for  $N$  Si atoms there are  $6N$  rings in the glass. In  $c$ - $\text{SiSe}_2$ , there are only 432 twofold rings for 216 Si atoms, i.e., two twofold rings per Si atom. In the glass the environment of Si atoms can be characterized into three categories: (1) Si

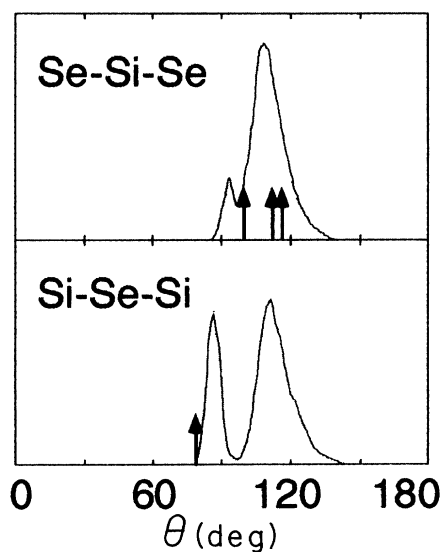


FIG. 3. Se-Si-Se and Si-Se-Si bond-angle distributions in  $\alpha$ - $\text{SiSe}_2$  (red curves). Crystalline angles (Ref. 1) are denoted by blue arrows.

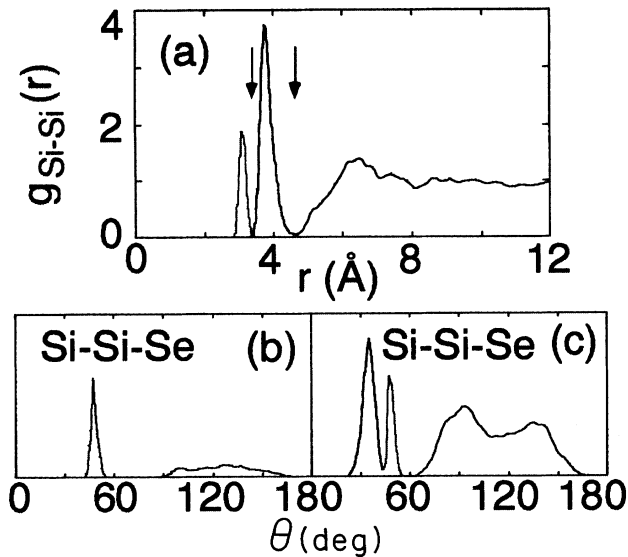


FIG. 4. (a) Partial Si-Si pair-correlation function in  $\alpha$ -SiSe<sub>2</sub>. Red peak and blue peak are due to twofold and threefold rings, respectively. (b) Si-Si-Se bond-angle distribution calculated with Si-Si cutoff of 3.4 Å [red arrow in (a)]. (c) The same as Fig. 4(b) with 4.6-Å Si-Si cutoff [blue arrow in (a)].

atoms that participate only in CS configurations. These Si atoms with no twofold rings are labeled as Si(0). (2) Si atoms that have only one twofold ring (tetrahedron sharing one edge). These are denoted by Si(1). (3) Si atoms that have two twofold rings, as in  $c$ -SiSe<sub>2</sub>, are labeled as Si(2). In the glass, there are 0.57 twofold rings per Si atom. Out of 124 twofold rings, there are 100 rings with Si(1)-type atom and the remaining 24 rings with Si(2)-type atom. Among the CS tetrahedra involving Si(0), the largest number of rings are threefold and eightfold. For Si(1)- and Si(2)-type atoms, the largest number of rings are twofold and eightfold. There is a predominance of eightfold rings among the larger rings.

Having analyzed the glass in terms of rings, let us now examine if there are chainlike molecular fragments in the glass. A molecular fragment is defined as an entity with three tetrahedra. The central tetrahedron contains a Si(2) atom, whereas the remaining two tetrahedra have Si(0), Si(1), or Si(2) atoms. There are six different types of frag-

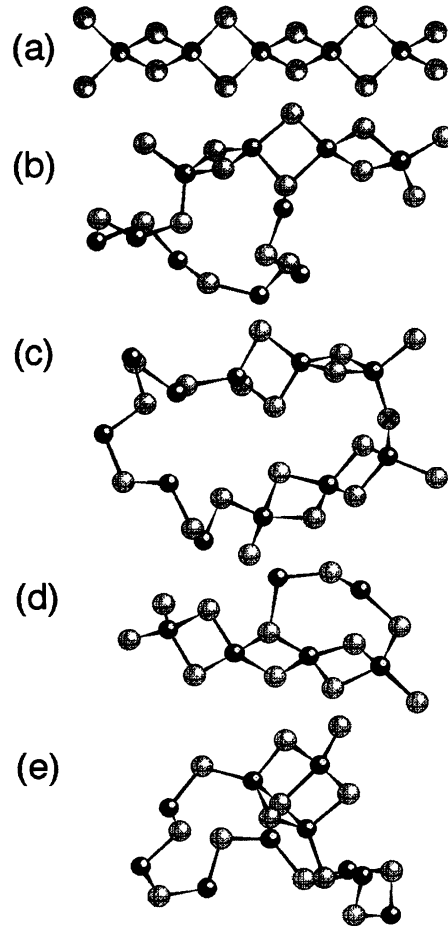


FIG. 5. (a) A chain of ES tetrahedra from crystalline SiSe<sub>2</sub>. Si(2), Si(1), and Si(0) atoms are represented by red, green, and cyan spheres. Se atoms are in yellow. Snapshots of tetrahedral molecular fragments and rings taken from a MD glass at 293 K are shown in (b) and (c). (b) 1-2-2-1 fragment, part of which is included in an eightfold ring. (c) Two 1-2-1 fragments in a ring. The crossed Se atom in (c) participates in a CS hinge configuration between two chainlike fragments. Snapshots from the MD liquid at 1293 K are shown in (d) and (e). (d) 1-2-2-1 fragment, part of which is in a fourfold ring. (e) Three interconnected twofold rings.

TABLE I. Distribution of rings in crystalline and glassy SiSe<sub>2</sub> for 216 Si atoms. Si(0) indicate corner-sharing configuration with no edge sharing, Si(1) share one edge, and Si(2) share two edges.

Ring size	02	03	04	05	06	07	08	09	10	11	12
Crystal											
Si(2)	432	0	0	0	0	0	0	0	0	0	0
Total rings/Si	2	0	0	0	0	0	0	0	0	0	0
Glass											
Si(0)	0	120	37	50	72	66	105	67	44	19	5
Si(1)	100	41	29	18	32	58	113	73	66	46	5
Si(2)	24	1	0	4	3	6	14	4	8	8	0
Total	124	162	66	72	107	130	232	144	118	73	10
Total rings/Si	0.57	0.75	0.31	0.33	0.50	0.60	1.07	0.67	0.55	0.34	0.04

TABLE II. Distribution of chainlike fragments in the rings in  $a$ - $\text{SiSe}_2$ .

Ring	0-2-0	0-2-2	1-2-0	1-2-1	1-2-2	2-2-2
3	0	0	0	1	0	0
4	0	0	0	0	0	0
5	0	0	2	0	0	0
6	0	0	5	1	0	0
7	0	0	3	1	0	0
8	0	0	2	13	0	0
9	0	0	3	4	0	0
10	0	0	3	4	1	0
11	0	0	2	7	3	0
12	0	0	0	0	1	0

ments: 0-2-0, 0-2-2, 1-2-0, 1-2-1, 1-2-2, 2-2-2, where 0-2-0 denotes a Si(0)-Si(2)-Si(0) fragment. Statistics of these fragments in threefold to twelfold rings are given in Table II. No fragments of type 0-2-0, 0-2-2, or 2-2-2 are found. The most commonly occurring fragments are 1-2-0 and 1-2-1. The latter occurs mostly in eightfold rings. The average length of these fragments is about 10–12 Å.

To look for the longest fragment, let us examine the fragment of type 1-2-2. By definition, a Si(2) must be surrounded on both sides by Si(1) or Si(2). Therefore, a 1-2-2 fragment must be a part of either 1-2-2-1 or 1-2-2-2. Since no 2-2-2 fragment is found, the latter does not exist in our system. The longest fragment in our glass is thus 1-2-2-1, which is about 15 Å.

Figure 5(a) shows the tetrahedral chain in  $c$ - $\text{SiSe}_2$ . Figures 5(b) and 5(c) show snapshots of fragments and rings taken from a MD glass at 293 K, while Figs. 5(d) and 5(e) are those in a MD liquid at 1293 K. Si(2), Si(1), and Si(0) atoms are represented by red, green, and cyan spheres, respectively. Se atoms are in yellow. Figure 5(a) is a 2-2-2-2-2 fragment. Figure 5(b) shows a 1-2-2-1 fragment, part of which is included in an eightfold ring. In Fig. 5(c), two 1-2-1 fragments are connected by a hinge made of the CS configuration (see the Se atom denoted by a cross). Contrary to the glass, in liquid  $\text{SiSe}_2$  the chainlike fragments have a broader distribution in rings of various sizes. Figure 5(d) depicts a 1-2-2-1 fragment, part of which is included in a fourfold ring. The liquid contains highly distorted structures. Figure 5(e) shows three interconnected twofold rings.

The relative population of Si(0), Si(1), and Si(2) atoms

has been determined using NMR measurements.<sup>13,14</sup> The existence of Si(0) in  $a$ - $\text{SiSe}_2$  has been proposed by Griffiths and co-workers.<sup>11,16</sup> Tenhover *et al.* determine Si(0), Si(1), and Si(2) to be 26%, 52%, and 22%, respectively.<sup>13</sup> Our MD result, 48% 46%, and 6%, shows that CS tetrahedra are more abundant in the MD glass when compared with the experiments on  $a$ - $\text{SiSe}_2$ . MD glasses are produced from the melt at a very rapid quench rate when compared with laboratory glasses. Since liquid has much more disorder than the glass, the MD glass shows more CS configuration, Si(0), and less Si(2) when compared with the experiment. Because of the rapid quenching rate of MD simulations, relaxation to more crystalline structures remains incomplete. On the other hand, the average length of ES chains, three units long, inferred from NMR data<sup>13</sup> is in favorable agreement with our simulation. It would be very useful to have experimental data on the population of Si(0), Si(1), and Si(2) in glasses prepared under different quench-rate conditions.

In summary, we have investigated the nature of tetrahedral-molecular fragments in glass by MD method. The results agree well with available experiments and reveal microscopic order in  $a$ - $\text{SiSe}_2$ .

We would like to thank Dr. David Price and Dr. Sherman Sussman for many valuable discussions. This research was supported by a grant from Louisiana Education Quality Support Fund Grant No. LEOSF-(1991-1992)-RD-A-05 and by National Science Foundation Grant No. ASC-9109906.

<sup>1</sup>J. Peters and B. Krebs, *Acta Crystallogr. B* **38**, 1270 (1982).

<sup>2</sup>G. Dittmar and H. Schafer, *Acta Crystallogr. B* **32**, 2726 (1976).

<sup>3</sup>J. A. E. Desa *et al.*, *J. Non-Cryst. Solids* **51**, 57 (1982).

<sup>4</sup>R. W. Johnson *et al.*, *J. Non-Cryst. Solids* **83**, 251 (1986); R. W. Johnson, *ibid.* **88**, 366 (1986); R. W. Johnson *et al.*, *Mater. Res. Bull.* **21**, 41 (1986).

<sup>5</sup>S. Susman *et al.*, *J. Non-Cryst. Solids* **125**, 168 (1990).

<sup>6</sup>A. C. Wright and A. J. Leadbetter, *Phys. Chem. Glasses* **17**, 122 (1976).

<sup>7</sup>A. J. Leadbetter and A. C. Wright, *J. Non-Cryst. Solids* **7**, 37 (1972).

<sup>8</sup>S. C. Moss and D. L. Price, in *Physics of Disordered Materials*, edited by D. Adler, H. Fritzsche, and S. R. Ovshinsky (Plenum, New York, 1985), p. 77.

<sup>9</sup>M. Tenhover *et al.*, *Solid State Commun.* **51**, 455 (1984).

<sup>10</sup>M. Tenhover *et al.*, *Phys. Rev. Lett.* **51**, 404 (1983).

<sup>11</sup>J. E. Griffiths *et al.*, *Phys. Rev. B* **30**, 6978 (1984).

<sup>12</sup>S. Sugai, *Phys. Rev. Lett.* **57**, 456 (1986).

<sup>13</sup>M. Tenhover *et al.*, *Solid State Commun.* **65**, 1517 (1988).

<sup>14</sup>K. Moran *et al.*, *Hyperfine Interact.* **62**, 55 (1990).

<sup>15</sup>The functional form of the potentials and a comprehensive discussion of the MD results are planned to be published elsewhere.

<sup>16</sup>Models of  $a$ - $\text{SiSe}_2$  based on CS and ES tetrahedra were proposed in Refs. 11 and 12. Such models were examined using computer-generated configurations using crystalline seeds by L. F. Gladden and S. R. Elliott, *Phys. Rev. Lett.* **59**, 908 (1987).

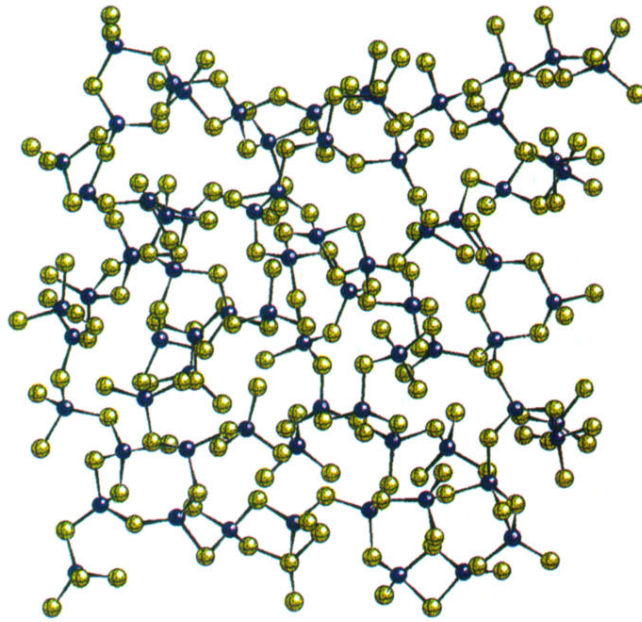


FIG. 1. Snapshot of a 9-Å-thick slice of a MD glass. Si atoms are indicated in blue and Se atoms in yellow.

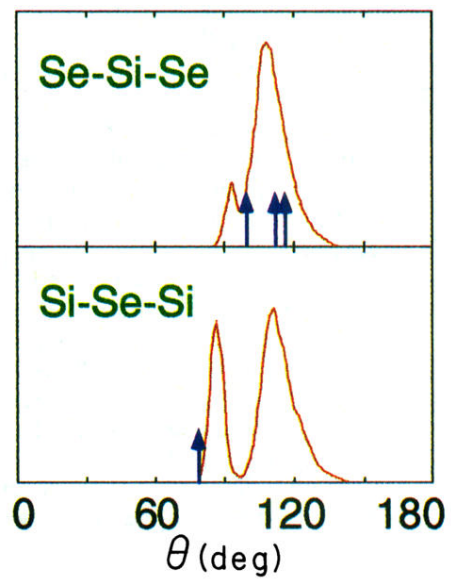


FIG. 3. Se-Si-Se and Si-Se-Si bond-angle distributions in  $\alpha$ -SiSe<sub>2</sub> (red curves). Crystalline angles (Ref. 1) are denoted by blue arrows.

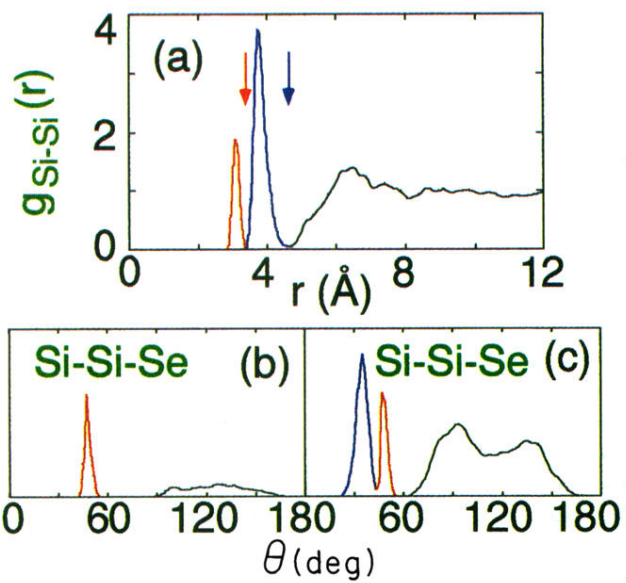


FIG. 4. (a) Partial Si-Si pair-correlation function in  $a\text{-SiSe}_2$ . Red peak and blue peak are due to twofold and threefold rings, respectively. (b) Si-Si-Se bond-angle distribution calculated with Si-Si cutoff of 3.4 Å [red arrow in (a)]. (c) The same as Fig. 4(b) with 4.6-Å Si-Si cutoff [blue arrow in (a)].

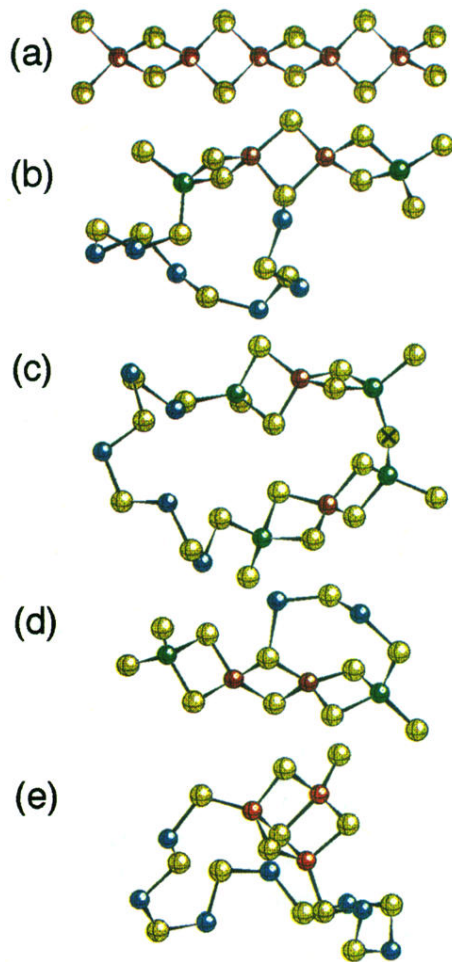


FIG. 5. (a) A chain of ES tetrahedra from crystalline SiSe<sub>2</sub>. Si(2), Si(1), and Si(0) atoms are represented by red, green, and cyan spheres. Se atoms are in yellow. Snapshots of tetrahedral molecular fragments and rings taken from a MD glass at 293 K are shown in (b) and (c). (b) 1-2-2-1 fragment, part of which is included in an eightfold ring. (c) Two 1-2-1 fragments in a ring. The crossed Se atom in (c) participates in a CS hinge configuration between two chainlike fragments. Snapshots from the MD liquid at 1293 K are shown in (d) and (e). (d) 1-2-2-1 fragment, part of which is in a fourfold ring. (e) Three interconnected twofold rings.